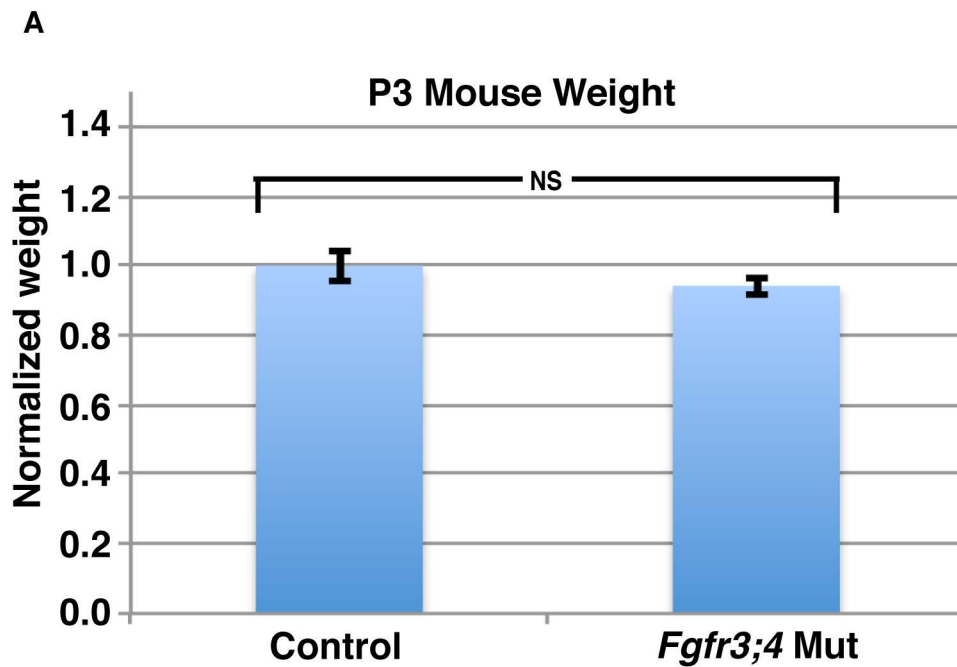


## FGF Receptors Control Alveolar Elastogenesis Supplementary information

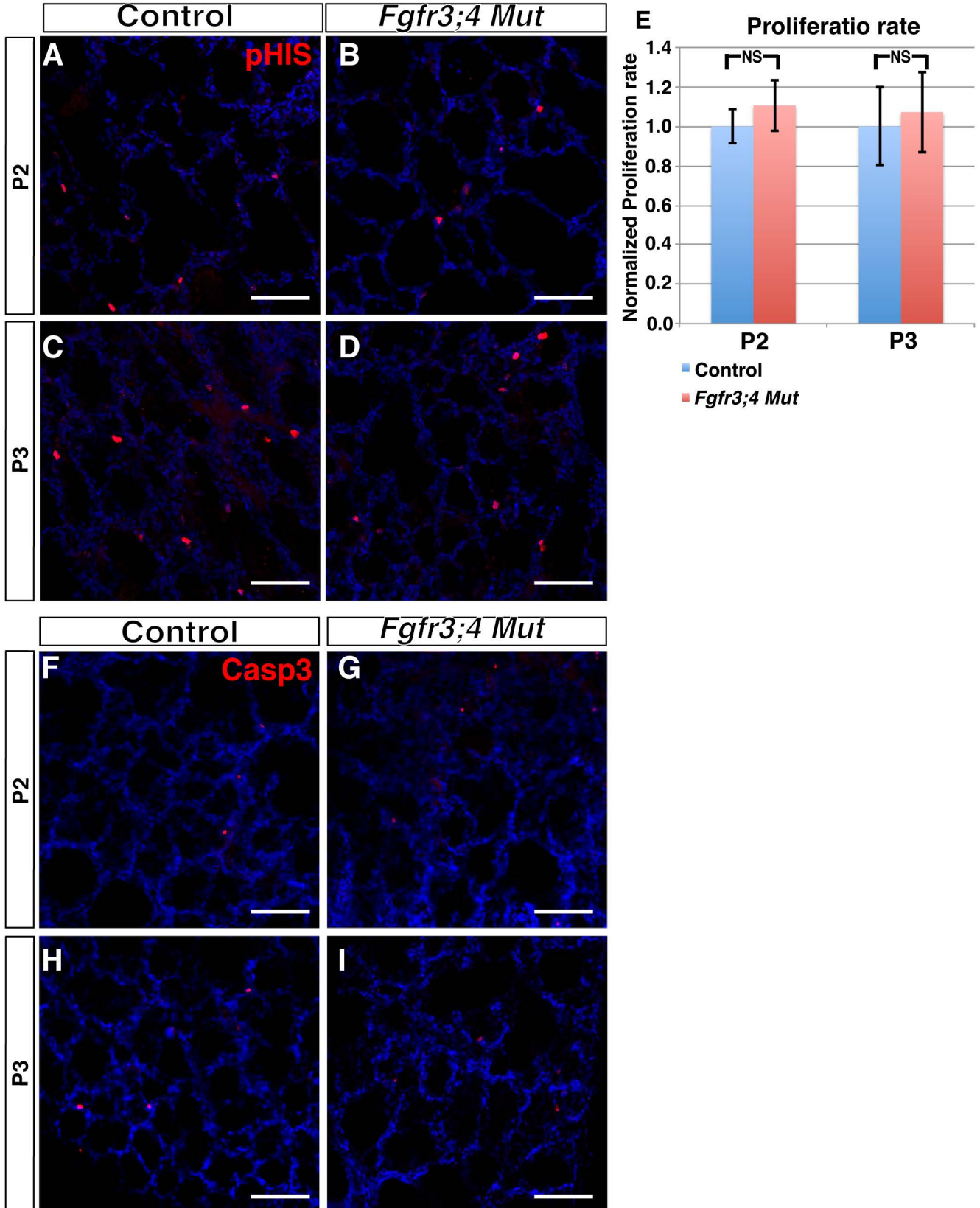
### Supplemental Figure 1



**Supplemental Figure 1.** Alveolar simplification in *Fgfr3;4* mutant lung is not preceded by an alteration in total mouse weight.

(A) Control and mutant mice were weighed at P3. There was no statistically significant difference between the mutant and control mouse weight at this stage. NS:  $p > 0.05$ . Data are presented as means ( $\pm$ SEM).

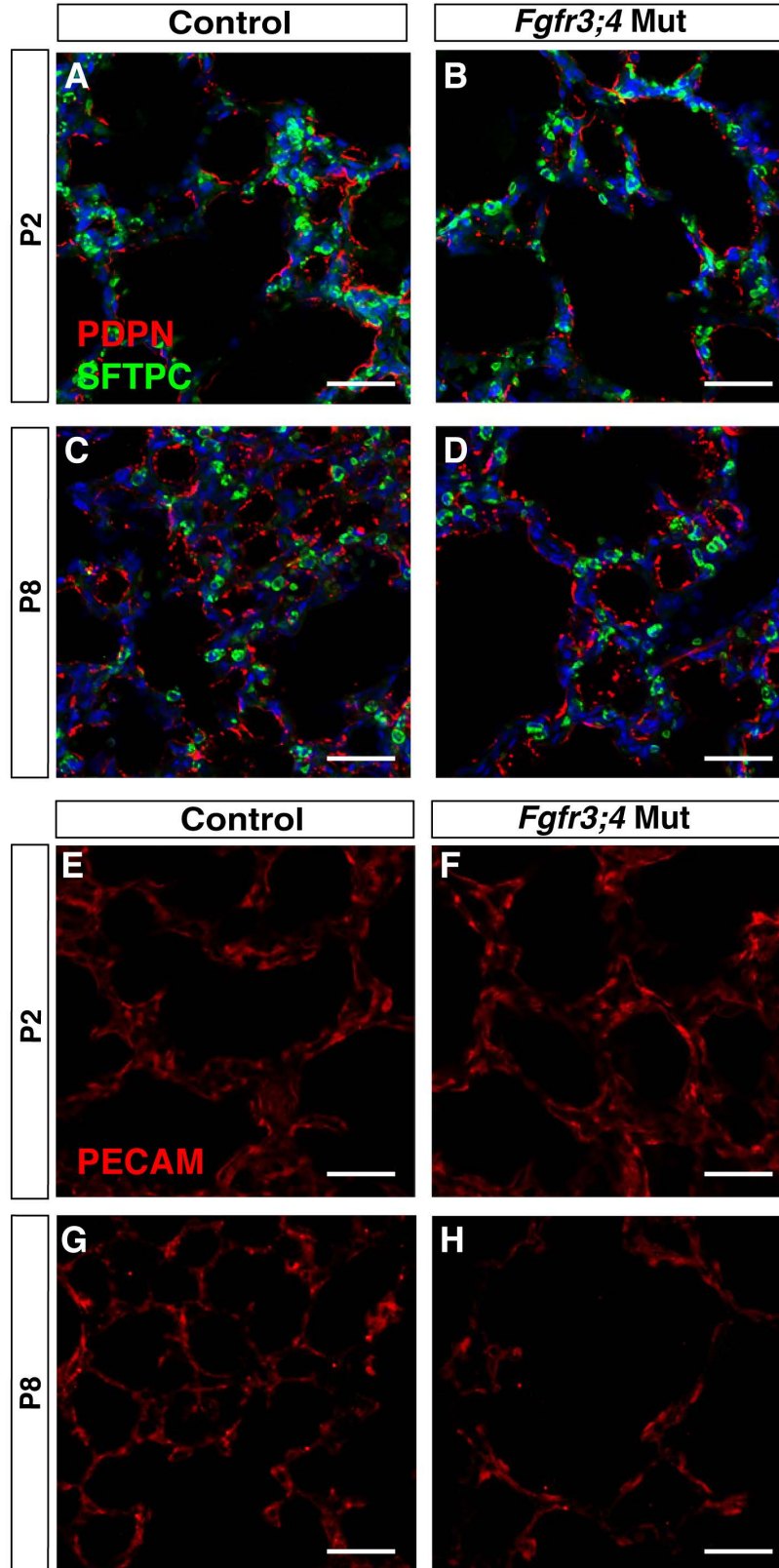
## Supplemental Figure 2



**Supplemental Figure 2.** Cell proliferation and cell death are not altered in *Fgfr3;4* mutant mice.

(A-D) Representative immunofluorescent staining for the proliferation marker pHIS (red) and nuclei Dapi (blue) at P2 and P3. (E) Quantification of the proliferation rate show that there is no statistically significant different in proliferation in the mutant compared to control at P2 and P3. NS:  $p > 0.05$ . Data are presented as means ( $\pm$ SEM). (F-I) Representative immunofluorescent staining for the cell death marker cleaved Casp3 (red) and nuclei Dapi (blue) at P2 and P3. At both stages, there was comparably few stained cells in mutant and control lungs. Scale bars: 100  $\mu$ m.

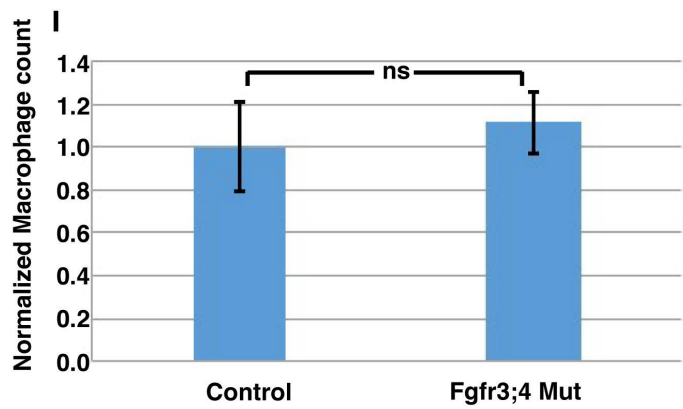
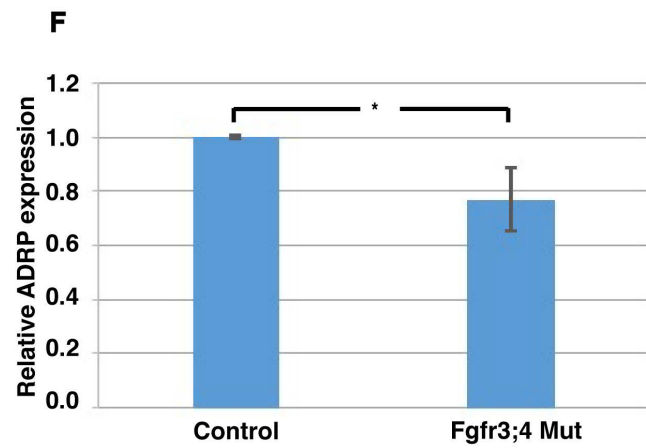
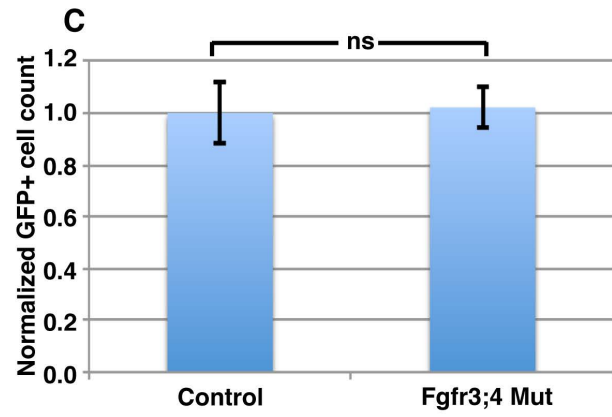
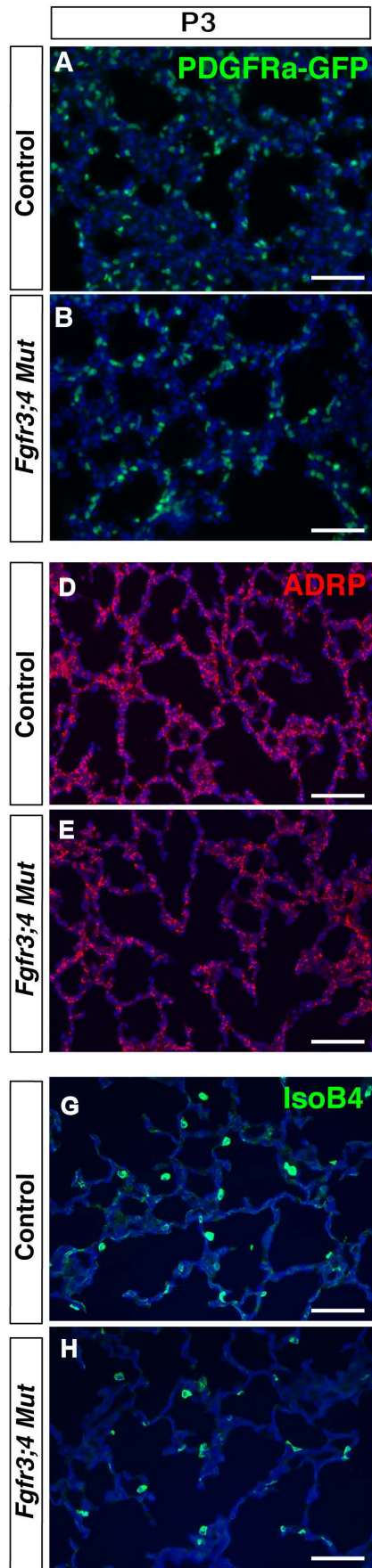
## Supplemental Figure 3



**Supplemental Figure 3.** The epithelial and endothelial lineages are normal in the *Fgfr3;4* mutant lungs.

(A-D) Representative immunofluorescent staining for alveolar type I cells (PDPN (red)) and alveolar type II cells (SFTPC (green)) in the alveolar region of P2 and P8 lungs. (E-H) Representative immunofluorescent staining for the capillary endothelial network (PECAM) in the alveolar region of P2 and P8 lungs. There is no change in the presence and distribution of these cell types in proportion to the complexity of the alveoli. Scale bars: 100  $\mu$ m.

## Supplemental Figure 4

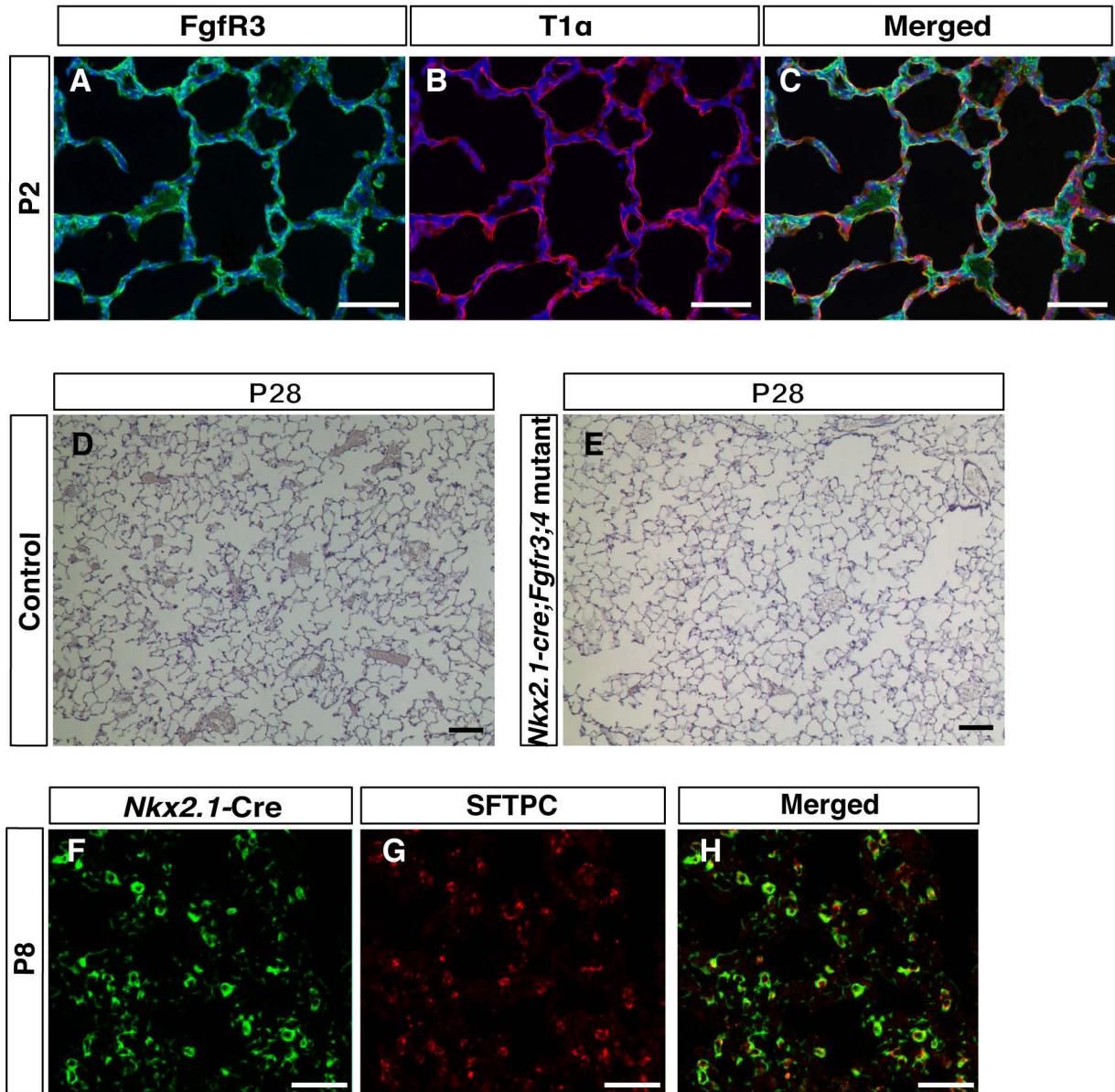




**Supplemental Figure 4.** *Fgfr3;4* mutant lungs exhibit normal number of PDGFRa+ cells, fewer lipofibroblasts and normal macrophages.

(A,B) Representative images of the alveolar region of PDGFRa-GFP positive cells (green) in the control (A) and mutant (B) lungs at P3. (C) Quantification revealed that the percentage of PDGFRa-GFP positive cells in total cells is unchanged in the mutant lung (n=3, p>0.05). (D,E) Representative images of the alveolar region stained with anti-ADRP antibody that labels lipid droplets in lipofibroblasts. (F) Quantification by pixel intensity in set areas indicates reduced expression of ADRP in the mutant as compared to control (n=3, p=0.029). (G,H) Representative images of the alveolar region stained with anti-IsoB4 antibody that labels macrophages. (I) Quantification revealed that the percentage of macrophages in total cells is unchanged in the mutant as compared to control (n=3, p=0.035). Data are presented as means ( $\pm$ SEM). Scale bars: 100  $\mu$ m.

# Supplemental Figure 5

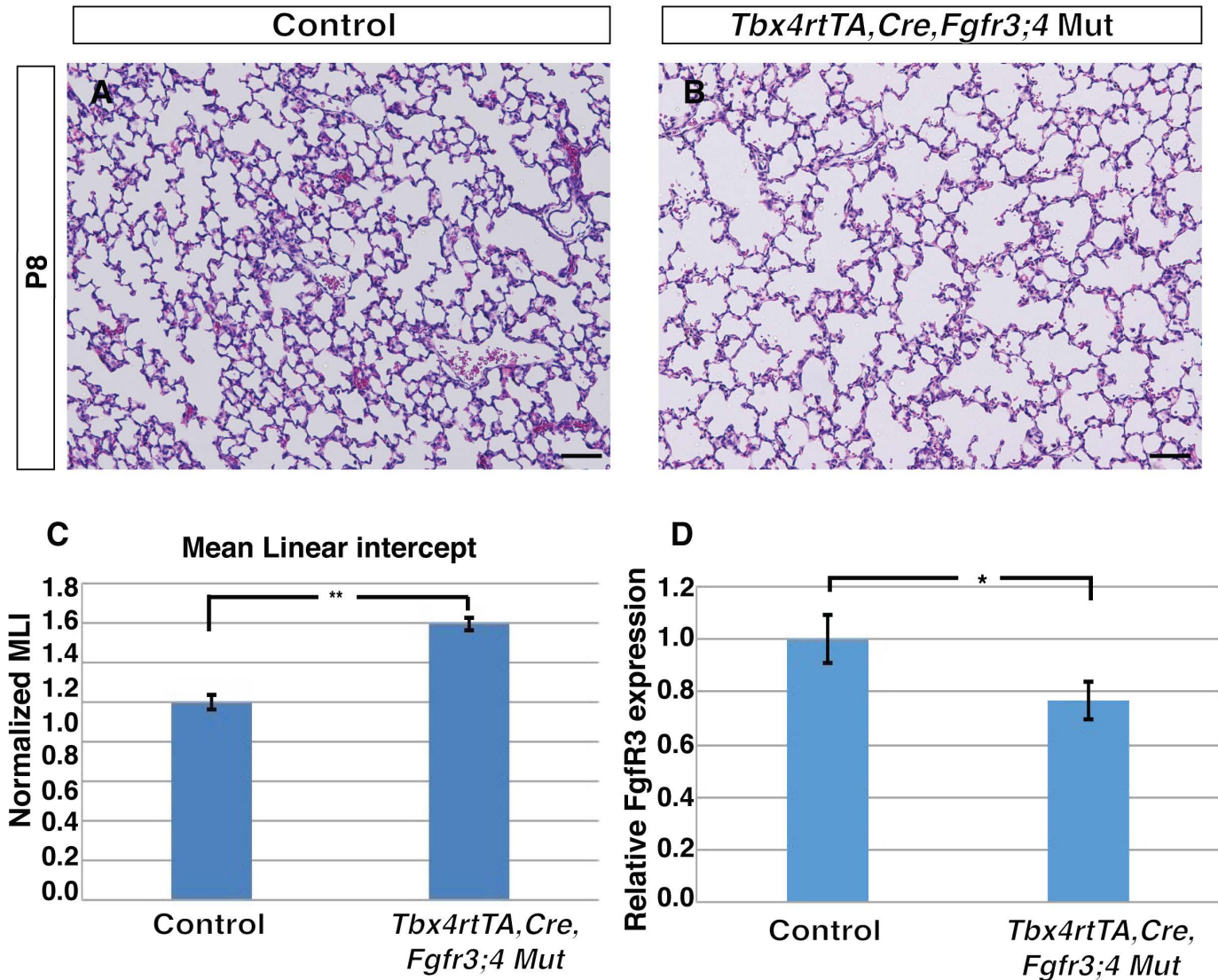


**Supplemental Figure 5.** *Nkx2-1-cre;Fgfr3;4* conditional mutants have normal lung despite robust *Nkx2-1-Cre* activity in the alveolar epithelium.

(A-C) Representative immunofluorescent staining for FGFR3 (green), T1 $\alpha$  (red) and nuclei Dapi (blue) at P2. Scale bars: 100  $\mu$ m. (D,E) Representative H&E stained sections of the alveolar regions of P28 lungs indicate that the *Nkx2-1-cre;Fgfr3;4* mutant showed normal morphology compared to control. (F-H) *Nkx2-1-Cre* activity, as reported by GFP reporter, is widespread in alveolar cells, including SFTPC-positive type II cells (red). Data are presented as means  $\pm$ SEM. Scale bars: 100  $\mu$ m.



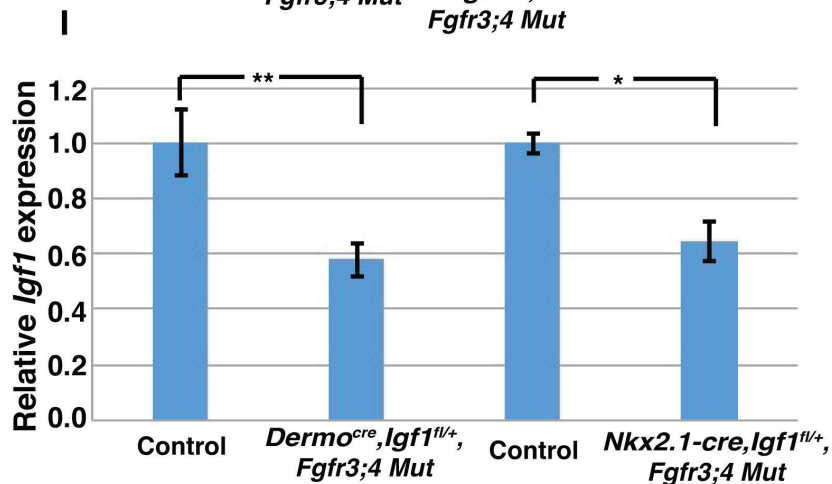
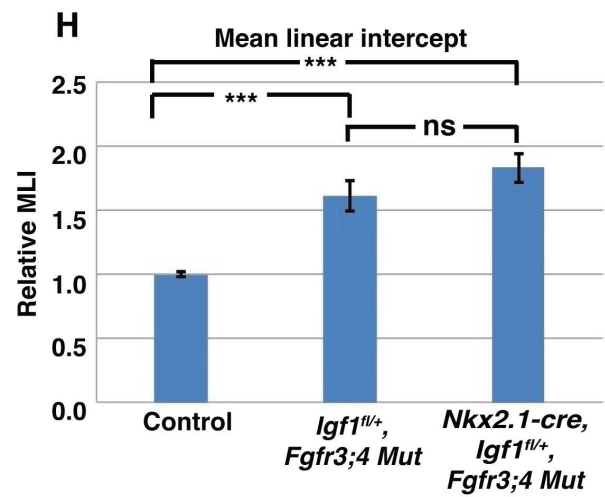
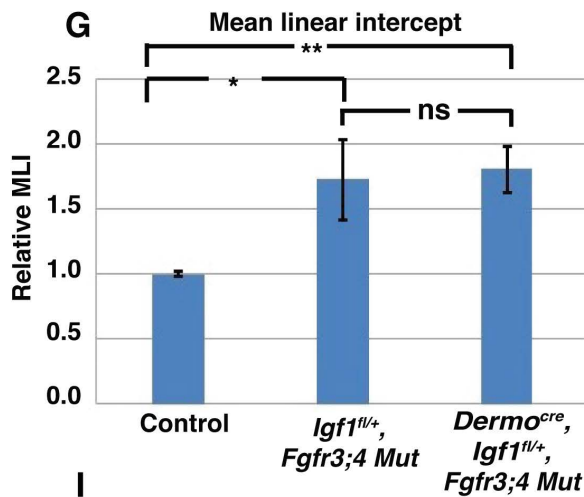
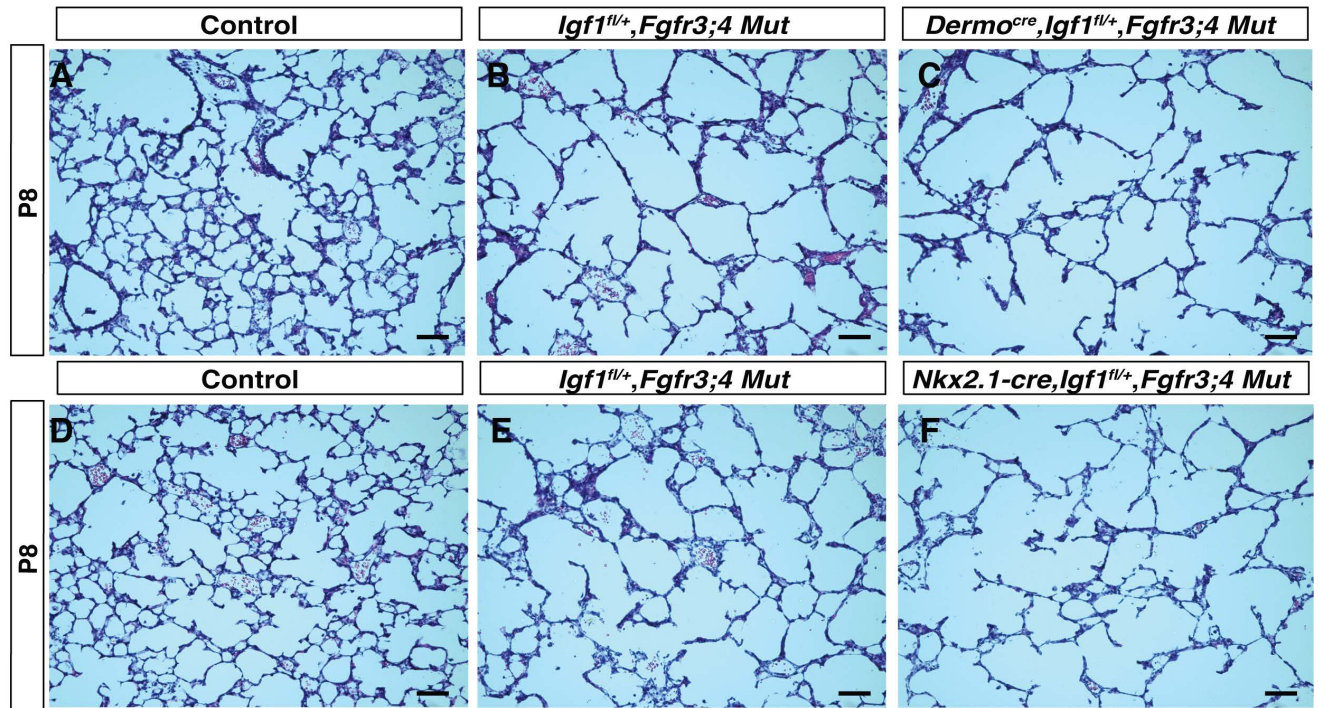
## Supplemental Figure 6



**Supplemental Figure 6.** Lung mesenchyme-specific inactivation of *Fgfr3;4* leads to alveolar simplification.

(A,B) Representative H&E stained sections from the alveolar regions of lungs at P8. (C) Quantification by MLI. *Fgfr3;4* mutant lungs showed a statistically significant increase in the relative MLI compared to control ( $p=0.005$ ,  $n=3$ ). (D) qRT-PCR analysis indicated a statistically significant decrease of *Fgfr3* expression in *Tbx4-rtTA; tetO-cre; Fgfr3;4* conditional lungs compared to control ( $p=0.02$ ,  $n=3$ ). Data are presented as means  $\pm$ SEM. Scale bars: 100  $\mu$ m.

## Supplemental Figure 7

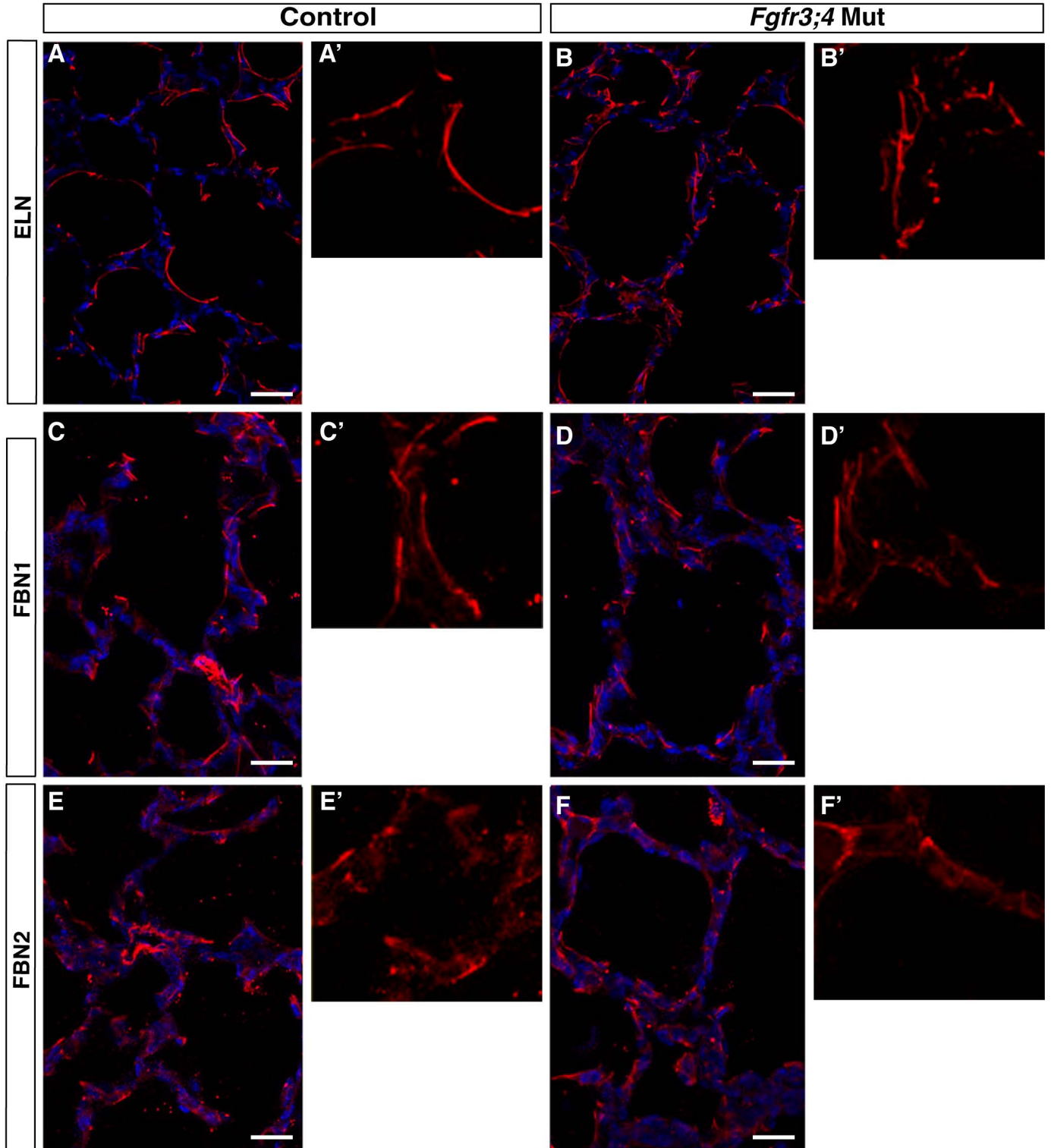


**Supplemental Figure 7.** Reduction of *Igf1* does not attenuate the alveolar simplification defect in global *Fgfr3;4* mutant.

(A-F) Representative H&E stained sections from the alveolar regions of P8 lungs with genotype as labeled. (G) Quantification by MLI. *Igf1<sup>fl/+</sup>;Fgfr3;4* mutant and *Dermo<sup>cre</sup>; Igf1<sup>fl/+</sup>;Fgfr3;4* mutant lungs both showed statistically significant increase in the relative MLI compared to control ( $p=0.0153$ ,  $n=3$  each; and  $p=0.0014$ ,  $n=3$  each, respectively). But the relative MLI was not significantly different between *Igf1<sup>fl/+</sup>;Fgfr3;4* mutant and *Dermo<sup>cre</sup>;Igf1<sup>fl/+</sup>;Fgfr3;4* mutant ( $p=0.725$ ,  $n=3$  each). (H) Quantification by MLI. *Igf1<sup>fl/+</sup>;Fgfr3;4* mutant and *Nkx2.1-cre;Igf1<sup>fl/+</sup>;Fgfr3;4* mutant lungs both showed statistically significant increase in the relative MLI compared to control ( $p=0.0008$ ,  $n=3$  each; and  $p=0.0002$ ,  $n=3$  each, respectively). But the relative MLI was not significantly different from *Igf1<sup>fl/+</sup>;Fgfr3;4* mutant and *Dermo-cre;Igf1<sup>fl/+</sup>;Fgfr3;4* mutant ( $p=0.072$ ,  $n=3$  each). (I) qRT analysis indicated that removing one allele of *Igf1* with *Nkx2.1-Cre* and *Dermo<sup>cre</sup>* resulted in 36% ( $p=0.03$ ,  $n=3$ ) and 42% ( $p=0.002$ ,  $n=3$ ) reduction of *Igf1* expression, respectively. Data are presented as means  $\pm$ SEM. Scale bars: 100  $\mu$ m.



# Supplemental Figure 8



**Supplemental Figure 8.** The microfibrer network is unaffected in the *Fgfr3;4* mutant lung.

(A-F, A'-F') Representative alveolar region of P2 lungs stained for Elastin (A,A',B,B'), Fibrillin 1 (C,C',D,D'), and Fibrillin 2 (E,E',F,F') (red) and Dapi for nuclei (blue). *Fgfr3;4* mutant lungs display disorganized Elastin, but similar patterns of Fibrillin 1 and Fibrillin 2 as compared to control. Scale bars: 100  $\mu$ m.

Table S1: Primers used for qPCR.

Target	Forward Primer (5'-3')	Reverse Primer (5'-3')
<i>Fbln4</i>	GGGCTACGAGCCTGATGAACA	GACTAGGGCGACAGTCATGC
<i>Fbln5</i>	TGTGCAACAGATTCCCACCA	TGGCCTTCCAGAAGCCAGTA
<i>Fbn1</i>	GATCAACGGCTACCCAAAAC	GTTGGCTTCCATCTCAGACC
<i>Fbn2</i>	AGGCAGAGGATGACGAAAACG	CTACGCTCTCCAGGCTGATTTG
<i>Emi1</i>	CTGCCAGCCGCCACAG	CCCAGCCACAGGGTTGATAG
<i>Emi2</i>	TCCATCCGCCCTGGTGTATC	AGGACAGCATCTCCATTCCAAC
<i>Mfap2</i>	GCCTCTTCTGCTGTTTCATGC	GTACTGGACATGGTCCGGGAAT
<i>Mfap5</i>	AGAAGGCCTTGCTGCTTGTCTT	ACATCATCTCCGCGTTGACCACT
<i>Lox</i>	GCCTGGCCAGTTCAGCATA	GGTGACAGCTGTGCCACTCC
<i>Loxl1</i>	CCTGCTTTTCAAGGAGAGACAAGG	TCTAACAACATCATGAAGTGCAGGAG
<i>Ltbp1</i>	AGCACCATCACCTCTGCTCT	CAGACACTGCTGTCTCTCAA
<i>Ltbp3</i>	ACGGCCTCAGTTGCATAGAC	AAAGAGCCTGGTGTGTTTCGT
<i>Ltbp4</i>	TGACCTCCGATAACAACACCA	AGGCAGAAAGCCTGTAGGTG
<i>Igf1</i>	TGGATGCTCTTCAGTTCGTG	TTTTGTAGGCTTCAGTGGGG
<i>Fgfr3</i>	TTGGTCTTTTGGTGTCTCTCC	TGAGGATGCGGTCTAAATCC